ORGANOMETALLICS

Article

pubs.acs.org/Organometallics

Versatile Coordination Behavior of Salicylaldehydethiosemicarbazone in Ruthenium(II) Carbonyl Complexes: Synthesis, Spectral, X-ray, Electrochemistry, DNA Binding, Cytotoxicity, and Cellular Uptake Studies

P. Kalaivani,[†] R. Prabhakaran,*[,†] P. Poornima,[‡] F. Dallemer,[§] K. Vijayalakshmi,[†] V. Vijaya Padma,[‡] and K. Natarajan*[,†]

[†]Department of Chemistry and [‡]Department of Biotechnology, Bharathiar University, Coimbatore-641 046, India

[§]Laboratoire Chimie Provence-CNRS UMR6264, Université of Aix-Marseille I, II and III-CNRS, Campus Scientifique de Saint-Jérôme, Avenue Escadrille Normandie-Niemen, F-13397 Marseille Cedex 20, France

Supporting Information

ABSTRACT: The reaction of salicylaldehydethiosemicarbazone, [H_2-(Sal-tsc)], with an equimolar amount of [RuHCl(CO)(PPh_3)$_3$] has afforded two complexes, namely [Ru(H-Sal-tsc)(CO)Cl-(PPh_3)$_2$] (**1**) and [Ru(Sal-tsc)(CO)(PPh_3)$_2$] (**2**), in one pot. The new complexes were separated and characterized by elemental analyses, various spectroscopic techniques (NMR, UV−vis, IR), X-ray crystallography, and cyclic voltammetry. In complex **1**, the ligand coordinated in a bidentate monobasic fashion by forming an unusual strained NS four-membered ring in 32% yield. However, in **2**, the ligand coordinated in a tridentate dibasic fashion by forming ONS five- and six-membered rings in 51% yield. Comparative biological studies such as DNA binding, cytotoxicity (MTT, LDH, and NO), and cellular uptake studies have been carried out for new ruthenium(II) complexes (**1** and **2**). From the DNA binding studies, it is inferred that the complex **1** exhibited electrostatic binding and **2** exhibited intercalative binding modes. On comparison of the cytotoxicity of the complexes in human lung cancer cells (A549) and liver cancer cells (HepG2), complex **2** exhibited better activity than **1**; this may be due to the strong chelation and subsequent electron delocalization in **2** increasing the lipophilic character of the metal ion into cells.

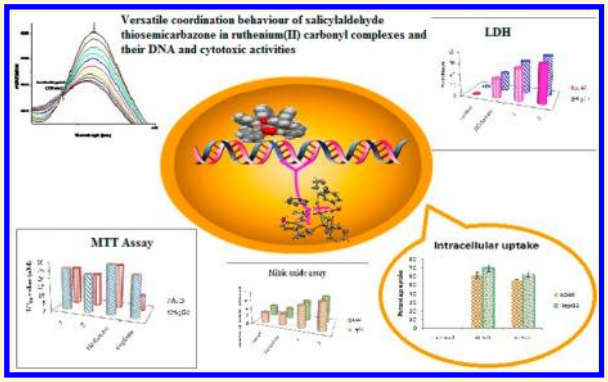

INTRODUCTION

Thiosemicarbazones are versatile ligands and adopt various binding modes with transition-metal and main-group-metal ions.[1] A number of reasons have been offered as responsible for their versatility in coordination, such as intramolecular hydrogen bonding, bulkier coligand, steric crowding on the azomethine carbon atom, and $\pi-\pi$ stacking interactions.[2] In addition, thiosemicarbazones and their metal complexes exhibit a wide range of applications that extend from their use in analytical chemistry through pharmacology to nuclear medicine.[3−6] Metal complexes that reveal the capacity to bind with nucleobases, DNA fragments, amino acids, peptides, and proteins are currently receiving special attention, mainly due to the clinical use of transition-metal complexes as antitumor drugs.[7−9] Platinum-based drugs have been in clinical use for cancer treatment for more than 30 years.[10] The landmark discovery of the antitumoral properties of cisplatin by Rosenberg in 1965 heralded a new area of anticancer research based on metallopharmaceuticals.[11] Although the mechanism by which cisplatin selectively kills cells is not entirely understood, it is generally believed that the therapeutic effects arise from covalent binding of the drug to DNA.[12] The efficacy of cisplatin, however, is reduced by increasing tumor resistance and high toxicity. These limitations have aroused interest toward the design and evaluation of transition-metal complexes other than platinum-based derivatives for therapeutic use. In recent years, several ruthenium-based complexes have been investigated for potential antitumor activity. Among the metal atoms used in anticancer metal complexes, ruthenium is the most unique. It is a rare noble metal unknown to living systems and has strong complexation ability with numerous ligands. In vitro and in vivo studies reveal that most ruthenium complexes bind covalently to DNA via the N-7 atom of purines and cause cytotoxicity by possibly inhibiting cellular DNA synthesis. Moreover, ruthenium complexes have a stronger affinity for cancer tissues than normal tissues. This is because ruthenium binds readily to transferrin molecules in plasma and is transported to the tumor cells. The first ruthenium compounds to be studied for cancer activity were chloro ammine

Received: September 28, 2012
Published: November 28, 2012

   dx.doi.org/10.1021/om300914n | *Organometallics* 2012, 31, 8323−8332

complexes: Durig et al. had observed in 1976 that the ruthenium(III) complex *fac*-[$Ru(NH_3)_3Cl_3$] induces filamentous growth of *E. coli* cells, at the same concentration as the required concentration of cisplatin for the same effect.[13] In 1980, this complex as well as the related ruthenium(II) complex *cis*-[$Ru(NH_3)_4Cl_2$] were evaluated for their anticancer properties by Clarke.[14] However, although active, these compounds were not soluble enough for pharmaceutical use.[15] In the following years, a large number of complexes were studied for their cytotoxic properties.[16−25] After extensive preclinical tests, the compounds [indH]*trans*-[Ru(*N*-ind)$_2$Cl$_4$] (KP1019) and [imiH]*trans*-[Ru(*N*-imi)(*S*-dmso)Cl$_4$] (NAMI-A) entered into clinical trials.[10] Ruthenium has therefore been considered to be an attractive alternative to platinum, in particular since many ruthenium compounds are not very toxic and some ruthenium compounds have been shown to be quite selective for cancer cells.[26,27] Along this line, herein we report the one-pot synthesis of new ruthenium(II) complexes containing salicylaldehyde thiosemicarbazone and their interactions with CT-DNA and anticancer activities (MTT, LDH and NO release) and a cellular uptake study against human lung (A549) and liver cancer cells (HepG2).

EXPERIMENTAL SECTION

Materials. The ligand [H_2-(Sal-tsc)] and the ruthenium metallic precursor [RuHCl(CO)(PPh_3)$_3$] were synthesized according to the standard literature procedures.[28−30] All the reagents used in this study were analar grade, and the solvents were purified and dried according to standard procedures.[31]

Preparation of New Ruthenium(II) Complexes. A solution of [H_2-(Sal-tsc)] (0.021 g; 0.105 mmol) in 10 cm^3 of benzene was added dropwise to a boiling solution of [RuHCl(CO)(PPh_3)$_3$] (0.100 g, 0.105 mmol) in benzene (10 cm^3). The mixture was heated at reflux for 5 h and was subjected to thin-layer chromatography. Two spots were identified and isolated by silica gel column chromatography by using 9/1 petroleum ether (60−80 °C)/ethyl acetate and 9/1 benzene/methanol mixtures as eluents, respectively, for complexes **1** and **2**.

*[Ru(H-Sal-tsc)(CO)Cl(PPh$_3$)$_2$] (**1**).* Anal. Calcd for $C_{45}H_{38}ClN_3O_2P_2RuS$: C, 61.19; H, 4.34; N, 4.76; S, 3.63. Found: C, 61.13; H, 4.31; N, 4.68; S, 3.57. Yield: 32%. Mp: 182 °C. FT-IR (cm^{-1}) in KBr: 3447 (ν_{O-H}), 1595 ($\nu_{C=N}$), 1285 (ν_{C-O}), 747 (ν_{C-S}), 1923 ($\nu_{C\equiv O}$) 1427, 1085, 696 cm^{-1} (for PPh_3). UV−vis (CH_2Cl_2), λ_{max}: 251 (15892), 268 (14789), 284 (9604) nm (dm^3 mol^{-1} cm^{-1}) (intraligand transition); 323 (8380), 371 (4961), 384 (2282), nm (dm^3 mol^{-1}cm^{-1}) (LMCT s → d). ^{1}H NMR (DMSO-d_6, ppm): 9.9 (s, 1H, −OH), 8.22 (s, 1H, −CH═N), 4.41 (s, −NH_2), 6.64−7.73 (m, aromatic). ^{13}C NMR (DMSO-d_6, ppm): 165.9 (C−S), 163.48 (C═N), 154.2 (aromatic PPh_3), 149.6 (aromatic PPh_3), 131.85 (aromatic PPh_3), 129.93 (2C, aromatic), 126.8 (aromatic), 123.8 (aromatic). ^{31}P NMR (DMSO-d_6, ppm): 36.03.

*[Ru(Sal-tsc)(CO)(PPh$_3$)$_2$] (**2**).* Anal. Calcd for $C_{45}H_{37}N_3SO_2P_2Ru$: C, 63.82; H, 4.40; N, 4.96; S, 3.79. Found: C, 63.78; H, 4.37; N, 4.92; S, 3.71. Yield: 51%. Mp: 216 °C. FT-IR (cm^{-1}) in KBr: 1575 ($\nu_{C=N}$), 1316 (ν_{C-O}), 745 (ν_{C-S}), 1949 ($\nu_{C\equiv O}$) 1435, 1089, 694 cm^{-1} (for PPh_3). UV−vis (CH_2Cl_2), λ_{max}: 248 (14,426), 269 (13862), 287 (10432) nm (dm^3 mol^{-1}cm^{-1}) (intraligand transition); 322 (7478), 378 (6308) nm (dm^3 mol^{-1} cm^{-1}) (LMCT s → d); 432 (4102) nm (dm^3 mol^{-1} cm^{-1}) forbidden (d → d) transition. ^{1}H NMR (DMSO-d_6, ppm): 8.44 (d, (J = 8.2 Hz), −CH═N), 6.68 (d, (J = 8.72 Hz), −NH_2), 7.2−7.63 (m, aromatic). ^{13}C NMR (DMSO-d_6, ppm): 166.4 (C−S), 164.24 (C═N), 155.2 (aromatic PPh_3), 150.2 (aromatic PPh_3), 131.98 (aromatic PPh_3), 130.03 (2C, aromatic), 127.2 (aromatic), 124.2 (aromatic). ^{31}P NMR (DMSO-d_6, ppm): 42.11.

Measurements. Infrared spectra were measured as KBr pellets on a Nicolet instrument between 400 and 4000 cm^{-1}. Elemental analyses of carbon, hydrogen, nitrogen, and sulfur were determined using a Vario EL III CHNS instrument at the Department of Chemistry, Bharathiar University, Coimbatore, India. The electronic spectra of the complexes have been recorded in dichloromethane using a Systronics 119 spectrophotometer in the 800−200 nm range. ^{1}H NMR, ^{13}C NMR, and ^{31}P NMR spectra were taken in DMSO at room temperature with a Bruker 400 MHz instrument with chemical shifts relative to tetramethylsilane (^{1}H, ^{13}C) and orthophosphoric acid (^{31}P). Cyclic voltammograms were recorded on a CH instrument by using a platinum-wire working electrode and platinum-disk counter electrode, with 0.1 M tetrabutylammonium perchlorate as supporting electrolyte at a scan rate of 100 mV s^{-1} in dichloromethane. All potentials were referenced to the standard Ag/AgCl electrode, and ferrocene was used as an external standard. Melting points were recorded by using a Lab India melting point apparatus.

X-ray Crystallography. Single crystals of [Ru(H-Sal-tsc)(CO)Cl-(PPh_3)$_2$] (**1**) and [Ru(Sal-tsc)(CO)(PPh_3)$_2$] (**2**) were obtained from a CH_2Cl_2/CH_3CN mixture and DMF, respectively. The data sets for the single-crystal X-ray studies for the new complexes were collected with Mo Kα (λ = 0.71073 Å) radiation on a Bruker SMART 1000 CCD diffractometer.[32] All calculations were performed using the SHELXS-97 and SHELXL-97 programs.[33,34]

DNA Binding Study. CT DNA solutions of various concentrations (0.05−0.5 μM) dissolved in a phosphate buffer (pH 7) were added to the new ruthenium(II) complexes (10 μM dissolved in a DMSO/H_2O mixture). Absorption spectra were recorded after equilibrium at 20 °C for 10 min. The intrinsic binding constant K_b was determined by using the Stern−Volmer equation (1).[35,36]

$$[DNA]/[\varepsilon_a - \varepsilon_f] = [DNA]/[\varepsilon_b - \varepsilon_f] + 1/K_b[\varepsilon_b - \varepsilon_f] \quad (1)$$

The absorption coefficients ε_a, ε_f, and ε_b correspond to A_{obsd}/[DNA], the extinction coefficient for the free complex and the extinction coefficient for the complex in the fully bound form, respectively. The slope and the intercept of the linear fit of the plot of [DNA]/[$\varepsilon_a - \varepsilon_f$] versus [DNA] give 1/[$\varepsilon_a - \varepsilon_f$] and 1/$K_b$[$\varepsilon_b - \varepsilon_f$], respectively. The intrinsic binding constant K_b can be obtained from the ratio of the slope to the intercept (Table 2).[36] Emission measurements were carried out by using a JASCO FP-6600 spectrofluorometer. Tris buffer was used as a blank to make preliminary adjustments. The excitation wavelength was fixed, and the emission range was adjusted before measurements. All measurements were made at 20 °C. For emission spectral titrations, the complex concentration was maintained constant at 10 μM and the concentration of DNA was varied from 0.05 to 0.5 μM. The emission enhancement factors were measured by comparing the intensities at the emission spectral maxima under similar conditions. In order to know the mode of attachment of CT DNA, fluorescence quenching experiments of EB-DNA were also carried out by adding 10 μL portions of 10 μM ruthenium(II) complexes every time to the samples containing 12 μM EB, 10 μM DNA, and Tris buffer (pH 7). Before the measurements, the system was shaken and incubated at room temperature for ∼5 min. The emission was recorded at 530−750 nm. On the basis of the classical Stern−Volmer equation, the quenching constant has been analyzed by using eq 2, where I_0 and I represent the fluorescence intensities in the absence and presence of the complexes, respectively, r is the concentration ratio of the complex to DNA, and K_{sq} is a linear Stern−Volmer quenching constant.

$$I_0/I = 1 + K_{sq}r \quad (2)$$

MTT (3-(4,5-Dimethylthiazol-2-yl)-2,5-diphenyltetrazolium Bromide) Assay. The effects of complexes **1** and **2** and the ligand on the viability of human lung cancer cells (A549) and liver cancer cells (HepG2) were determined by the 3-(4,5-dimethylthiazol-2-yl)-2,5-diphenyltetrazolium bromide (MTT) assay.[37] The cells were seeded at a density of 10000 cells per well in 200 μL of RPMI 1640 medium and were allowed to attach overnight in a CO_2 incubator, and then the complexes dissolved in DMSO were added to the cells at final concentrations of 1, 10, 25, and 50 μM in the cell culture media. After

dx.doi.org/10.1021/om300914n | *Organometallics* 2012, 31, 8323−8332

Scheme 1. Preparation of New Ruthenium(II) Complexes

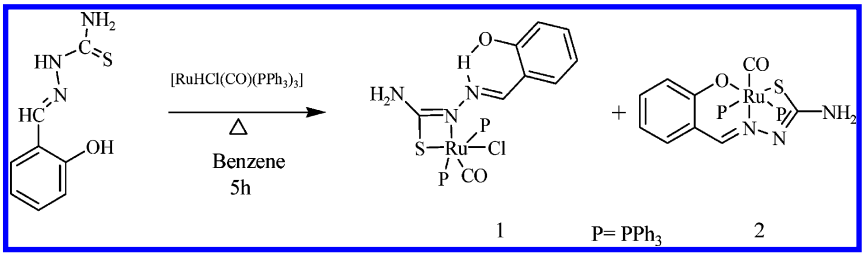

48 h, the wells were treated with 20 μL of MTT (5 mg/mL PBS) and incubated at 37 °C for 4 h. The purple formazan crystals that formed were dissolved in 200 μL of DMSO and read at 570 nm in a micro plate reader.

Release of Lactate Dehydrogenase (LDH). LDH activity was determined by the linear region of a pyruvate standard graph using regression analysis and expressed as percentage (%) leakage as described previously.[38] Briefly, in a set of tubes, 1 mL of buffered substrate (lithium lactate) and 0.1 mL of the media or cell extract were added and the tubes were incubated at 37 °C for 30 min. After 0.2 mL of NAD solution was added, the incubation was continued for another 30 min. The reaction was then arrested by adding 0.1 mL of DNPH reagent, and the tubes were incubated for a further 15 min at 37 °C. After this, 0.1 mL of media or cell extract was added to blank tubes after arresting the reaction with DNPH. A 3.5 mL portion of 0.4 N sodium hydroxide was added to all the tubes. The intensity of the color that developed was measured at 420 nm in a Shimadzu UV/visible spectrophotometer. The amount of LDH released was expressed as a percentage.

Nitric Oxide (NO) Assay. The amount of nitrite was determined by the method of Stueher and Marletta.[39] Nitrite reacts with Griess reagent to give a colored complex measured at 540 nm. To 100 μL of the medium was added 50 μL of Griess reagent I, and these were mixed and allowed to react for 10 min. This was followed by 50 μL addition of Griess reagent II, and the reaction mixture was mixed well and incubated for another 10 min at room temperature. The pink color that developed was measured at 540 nm in a microquant plate reader (Biotek Instruments).

Cellular Uptake Study. Cellular uptakes of complexes **1** and **2** and the ligand were quantified according to the literature method with a slight modification.[40] Briefly, the lung (A549) and liver (HepG2) cancer cells were treated with the test compounds for a period of 2 h. The medium was aspirated, and cells were washed three times with ice cold PBS. Then the cells were lysed with PBS containing 1% Triton X-100. Concentration of the complexes and the ligand in the cell lysates was measured with a fluorescence spectrophotometer (Jasco FP 6600) at their maximum excitation/emission wavelengths of 492/530, 426/495 and 220/291 nm, respectively, for complexes **1**, **2** and ligand. To offset the background fluorescence from the cellular components, separate standardization curves were prepared using cellular lysates containing series of known concentrations of different complexes and the intracellular concentrations were determined using the standard curve.

RESULTS AND DISCUSSION

Reaction of $[H_2\text{-(Sal-tsc)}]$ with an equimolar amount of $[RuHCl(CO)(PPh_3)_3]$ resulted in two different entities with different structural features in a single reaction (Scheme 1). The new complexes are soluble in common organic solvents such as dichloromethane, chloroform, benzene, acetonitrile, ethanol, methanol, dimethyl sulfoxide, and dimethylformamide. The analytical data of the complexes agreed well with the proposed molecular formulas.

Spectroscopic Studies. The IR spectrum of $[H_2\text{-(Sal-tsc)}]$ shows a sharp band at 1611 cm^{-1} corresponding to the $\nu_{C=N}$ vibration of the azomethine group. In the IR spectra of the new complexes **1** and **2**, this band has been observed at 1575 and 1595 cm^{-1}, indicating the coordination of the azomethine nitrogen atom to the ruthenium.[41,42] A sharp band that appeared for the ligand at 826 cm^{-1} corresponding to a $\nu_{C=S}$ vibration disappeared completely in both of the complexes, and a new band appeared at 745 and 747 cm^{-1} corresponding to a possible ν_{C-S} vibration, indicating coordination of a thiolate sulfur atom after enolization followed by deprotonation.[43,44] A broad band corresponding to a ν_{OH} vibration that appeared at 3439 cm^{-1} in the ligand has been observed at 3447 cm^{-1} in complex **1**, indicating the nonparticipation of the phenolic oxygen atom in coordination.[45] However, this band completely disappeared in complex **2**, indicating the involvement of phenolic oxygen in coordination. This was further supported by an increase in the phenolic C−O stretching frequency, appearing at 1316 cm^{-1}. Sharp bands at 1923 and 1949 cm^{-1} account for the terminal carbonyl group in **1** and **2**, respectively. In addition, vibrations corresponding to the presence of triphenylphosphine also appeared in the expected region.[46] The electronic spectra of the complexes have been recorded in dichloromethane, and they displayed six bands in the region around 248−432 nm. The bands appearing in the region 248−287 nm have been assigned to intraligand transitions,[47] the bands around 322−384 nm have been assigned to ligand to metal charge transfer transitions, and the band 432 nm has been assigned to a forbidden (d → d) transition. The ^1H NMR spectra of $[H_2\text{-(Sal-tsc)}]$ and complexes **1** and **2** showed a complex overlap of signals in the δ 6.3−7.6 ppm range corresponding to aromatic protons of the ligand and coordinated triphenylphosphine.[42] A sharp singlet appearing for complex **1** at δ 8.21 ppm corresponds to azomethine protons of the ligand.[43] For complex **2**, a doublet corresponding to the azomethine group was observed at δ 8.44 ppm, due to the coupling with the phosphorus atom of the triphenylphosphine.[48] In the spectra of the ligand the singlet appearing at δ 9.52 ppm is assigned to the N(2)HCS group.[49] However, in the spectra of the complexes there was no resonance attributable to N(2)H, indicating the coordination of ligand in the anionic form upon deprotonation at N(2). A sharp singlet corresponding to the phenolic −OH group appeared at δ 11.25 ppm in the free ligand. In the spectra of **1**, the appearance of a singlet at δ 9.9 ppm indicated the non-participation of the phenolic oxygen in coordination,[50] and this signal completely disappeared in **2**, confirming the involvement of the phenolic oxygen in coordination. Though the spectra of **1** showed a singlet at δ 4.41 ppm corresponding to NH_2 protons, the same has been observed as a doublet at δ 6.68 ppm for **2**, which may be due to the restricted C═N bond rotation of the ligand.[48] In the $^{13}C\{^1H\}$ NMR spectra of the complexes, the thioamide (C−S) carbon resonates at 166 and 167.0 ppm. The azomethine carbon resonance is observed at 164.0 and 163.48 ppm. In both complexes, aromatic carbon atoms of the

dx.doi.org/10.1021/om300914n | Organometallics 2012, 31, 8323−8332

phenoxy group observed around 129.4, 126.8, 123.8 ppm (complex **1**) and 130.02, 127.2, 124.2 ppm (complex **2**) are comparable to the literature values.[51] The C≡O carbon resonating at 208 ppm (**1**) and 207 ppm (**2**) is comparable with earlier observations.[4] In both complexes three signals corresponding to the presence of triphenylphosphine observed at 154.2, 149.6, and 131.28 ppm (complex **1**) and 155.4, 150.2, and 131.98 ppm (complex **2**) are in the range of the reported values.[52] In order to confirm the presence of triphenylphosphine, ^{31}P NMR spectra were recorded. The singlet observed at 36.03 and 42.11 ppm in complexes **1** and **2**, respectively, suggested the presence of two magnetically equivalent triphenylphosphines trans to each other (Figure S1 and S2, Supporting Information).

X-ray Crystallography. Complexes **1** and **2** crystallized in monoclinic space group *C*2/*c*. The crystallographic data of the complexes are given in Table S1 (Supporting Information). The molecular structures and hydrogen-bonding diagrams are depicted in Figures 1−4. In complex **1**, the ligand [H_2-(Sal-tsc)] is coordinated to ruthenium ion through the N(2) nitrogen and thiolate sulfur atoms, forming a more strained four-membered chelate ring with a bite angle N(2)−Ru(1)−S(1) of 65.1(1)°. The Ru(1)−N(2) bond distance is 2.208(5) Å, and the Ru(1)−S(1) distance is 2.413(1) Å. The other four sites are occupied by phosphorus atoms of two triphenylphosphine ligands which are mutually trans to each other with Ru(1)−P(1) and Ru(1)−P(2) distances of 2.384(1) and 2.380(1) Å and one chloride and a carbonyl group with Ru(1)−Cl(1) and Ru(1)−C(9) distances of 2.427(1) and 1.835(5) Å, respectively. The observed bond distances are comparable with those found in other reported ruthenium complexes containing PPh_3.[53] The cis angles N(2)−Ru(1)−P(2) = 89.7(1)°, N(2)−Ru(1)−P(1) = 88.9(1)°, P(1)−Ru(1)−S(1) = 89.42(4)°, and P(2)−Ru(1)−Cl(1) = 89.10(5)° are acute, whereas the other cis angles C(9)−Ru(1)−P(1) = 91.4(1)°, C(9)−Ru(1)−P(2) = 90.1(1)°, C(9)−Ru(1)−S(1) = 101.3(1)°, P(2)−Ru(1)−S(1) = 90.68(4)°, C(9)−Ru(1)−Cl(1) = 94.5(1)°, N(2)−Ru(1)−Cl(1) = 99.2(1)°, and P(1)−Ru(1)−Cl(1) = 90.40(5)° are obtuse. The trans angles C(9)−Ru(1)−N(2) = 166.4(2)°, P(2)−Ru−P(1) = 178.48(5)°, and S(1)−Ru(1)−Cl(1) = 164.23(5)° deviate from linearity. The variations in bond lengths and angles lead to a significant distortion from an ideal octahedral geometry for the complex.

In addition, complex **1** contains one intramolecular hydrogen bond through the hydrogen atom of the hydroxy group with the hydrazinic nitrogen (N3) of thiosemicarbazone moiety with an O1(A)−H(A)···N3(A) distance of 2.680 Å and one intermolecular hydrogen bond through the hydrogen atom of the amine nitrogen (N1) of one molecule with the oxygen

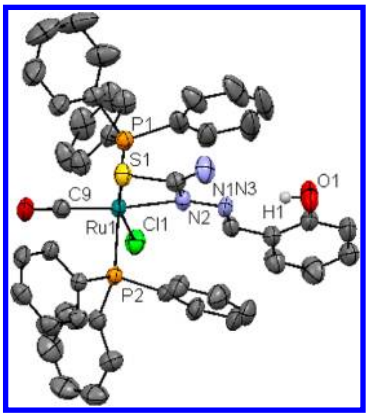

Figure 1. ORTEP diagram of [Ru(H-Sal-tsc)(CO)Cl(PPh_3)$_2$] (**1**) (hydrogen atoms are omitted for clarity). Bond lengths (Å): Ru(1)−N(1), 2.192(2); Ru(1)−P(1), 2.3815(7); Ru(1)−P(2), 2.3703(7); Ru(1)−S(1), 2.4012(7); Ru(1)−Cl(1), 2.4247(7); Ru(1)−C(37), 1.845(3). Bond angles (deg): C(9)−Ru(1)−N(2), 166.4(2); C(9)−Ru(1)−P(2), 90.1(1); N(2)−Ru(1)−P(2), 89.7(1); C(9)−Ru(1)−P(1), 91.4(1); N(2)−Ru(1)−P(1), 89.9(1); P(2)−Ru(1)−P(1), 178.48(5); C(9)−Ru(1)−S(1), 101.3(1); N(2)−Ru(1)−S(1), 65.1(1); P(2)−Ru(1)−S(1), 90.68(4); P(1)−Ru(1)−S(1), 89.42(4); C(9)−Ru(1)−Cl(1), 94.5(1); N(2)−Ru(1)−Cl(1), 99.2(1); P(2)−Ru(1)−Cl(1), 89.10(5); P(1)−Ru(1)−Cl(1), 90.40(5); S(1)−Ru(1)−Cl(1), 164.23(5).

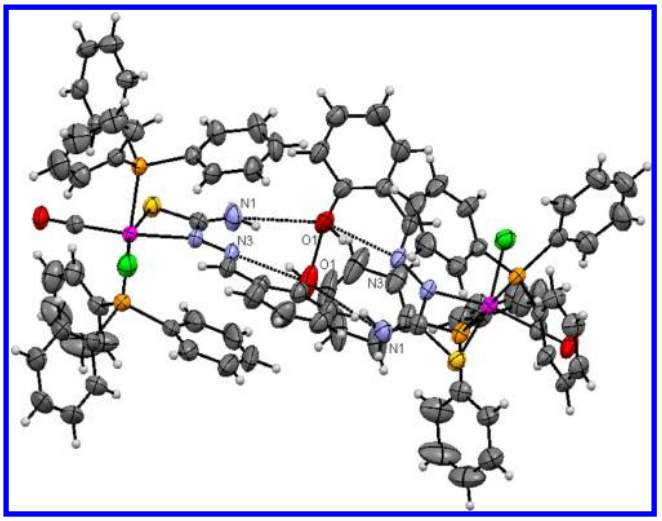

Figure 2. ORTEP diagram of **1** with hydrogen bonds leading to a pseudo-hydroxo-bridged binuclear structure.

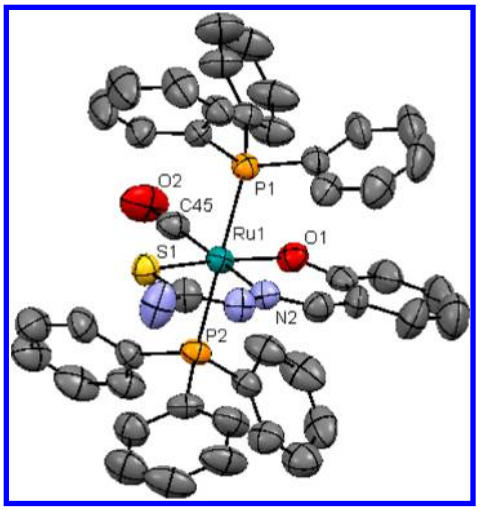

Figure 3. ORTEP diagram of [Ru(Sal-tsc)(CO)(PPh_3)$_2$] (**2**) (hydrogen atoms are omitted for clarity). Bond lengths (Å): Ru(1)−N(2), 2.061(6); Ru(1)−P(1), 2.406(2); Ru(1)−P(2), 2.399(2); Ru(1)−S(1), 2.344(2); Ru(1)−O(1), 2.069(5); Ru(1)−C(37), 1.893(8). Bond angles (deg): C(45)−Ru(1)−O(1), 95.0(3); C(45)−Ru(1)−N(2), 174.0(3); O(1)−Ru(1)−N(2), 90.6(2); C(45)−Ru(1)−S(1), 93.3(2); O(1)−Ru(1)−S(1), 171.8(1); N(2)−Ru(1)−S(1), 81.2(2); C(45)−Ru(1)−P(1), 87.4(2); N(2)−Ru(1)−P(1), 90.7(2); S(1)−Ru(1)−P(1), 94.29(7); C(45)−Ru(1)−P(2), 91.2(2); O(1)−Ru(1)−P(2), 92.0(1); N(2)−Ru(1)−P(2), 90.9(2); S(1)−Ru(1)−P(2), 87.73(7); P(1)−Ru(1)−P(2), 177.58(7).

dx.doi.org/10.1021/om300914n | *Organometallics* 2012, 31, 8323−8332

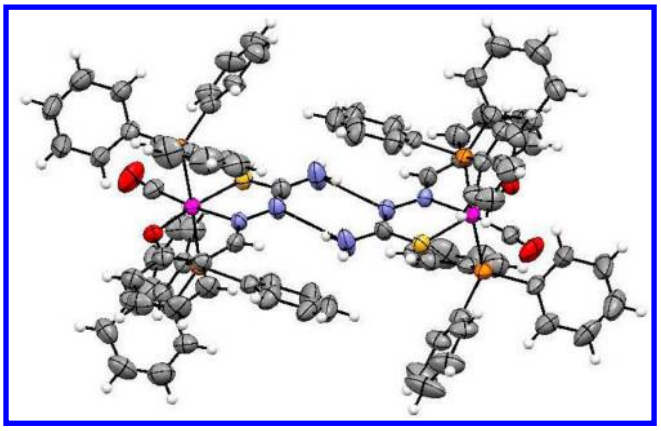

Figure 4. ORTEP diagram of **2** with hydrogen bonds leading to a pseudo-binuclear structure.

atom of the hydroxyl group (O1) of another molecule with an N1(A)−H(A)···O1(B) distance of 3.054 Å, leading to the formation of a pseudo-hydroxo-bridged binuclear complex (Table 1, Figure 2).

Table 1. Hydrogen Bonds for Complexes 1 and 2 (Å and deg)

D−H···A	*d*(D−H)	*d*(H···A)	*d*(D···A)	∠(DHA)
Complex **1**[a]				
O1(A)−H1(A)···N3(A)	0.850	1.95(2)	2.680	143.16
N1(A)−H1(A)···O1(B)	0.860	2.27(4)	3.05(4)	150.81
N1(B)−H1(B)···O1(A)	0.860	2.27(4)	3.05(4)	150.81
Complex **2**[b]				
N3(A)−H(A)···N1(B)	0.861	2.16(2)	2.98(8)	160.84
N3(B)−H(B)···N1(A)	0.861	2.16(2)	2.98(8)	160.84
N9(A)−H(A)···N4(B)	0.859	2.17(9)	2.99(3)	158.18
N6(B)−H(B)···N7(A)	0.860	2.15(1)	2.99(5)	167.20
N6(A)−H(A)···N7(B)	0.860	2.15(1)	2.99(5)	167.20
N9(B)−H(B)···N4(A)	0.859	2.17(9)	2.99(3)	158.18

[a]Symmetry operation: (x, y, z); $(1 - x, y, 1.5 - z)$. [b]Symmetry operation: (x, y, z); $(1 - x, y, {}^{1}/_{2} - z)$.

Suitable crystals of complex **2** were obtained from dimethylformamide. Complex **2** crystallized in the monoclinic crystal system with three independent molecules in the unit cell. In this complex, the thiosemicarbazone ligand coordinated to ruthenium in an ONS fashion by utilizing its phenolic oxygen, N1 hydrazinic nitrogen, and thiolate sulfur atoms with the formation of one six-membered ring and another five-membered ring with a bite angle N(2)−Ru(1)−S(1) of 81.2(2)°.

However, on comparison with complex **1**, the angular distortion observed in **2** is much less, which may be due to strong ONS chelation of the ligand. The Ru(1)−N(2) bond distance is 2.061(6) Å, the Ru(1)−O(1) bond distance is 2.069(5) Å, and the Ru(1)−S(1) distance is 2.344(2) Å. The other three sites are occupied by phosphorus donor atoms of two triphenylphosphines with Ru(1)−P(1) and Ru(1)−P(2) distances of 2.406(2) and 2.399(2) Å, respectively, and one carbonyl group with a Ru(1)−C(45) distance of 1.893(8) Å. These values are comparable with those found for complexes reported earlier.[54] The trans angles C(45)−Ru(1)−N(2) = 174.0(3)°, O(1)−Ru(1)−S(1) = 171.8(1)°, and P(1)−Ru−P(2) = 177.58(7)° indicate a significant distortion in the octahedral geometry of the complex. In this complex, one of the hydrogen atoms of each amino group of three independent molecules (N3, N6, and N9) are engaged in intermolecular hydrogen bonding with the hydrazinic nitrogen atoms (N1, N7, and N4) of a second set of three molecules: N3(A)−H(A)···N1(B) and N3(B)−H(B)···N1(A), N6(A)−H(A)···N7(B) and N9(B)−H(B)···N4(A), N9(A)−H(A)···N4(B) and N6(B)−H(B)···N7(A) (Table 1). This intermolecular hydrogen bonding creates a pseudo-binuclear structure (Figure 4).

Salicylaldehyde thiosemicarbazone exists in thiol and thione forms as indicated by II and III, and they can form stable five- and six-membered rings as in VI and VII. However, the coordination behavior of salicylaldehyde thiosemicarbazone was reported by Bhattacharya et al., who stated that the formation of a five-membered ring is an impossible mode of binding and a four-membered ring is possible.[50,53] They supported the formation of a four-membered ring as in VIII by offering a couple of reasons: intramolecular hydrogen bonding and a bulky coligand or bulky substitution on the azomethine carbon atom. In contrast to this, we observed both five- and four-membered-ring products from a single reaction between salicylaldehyde thiosemicarbazone and $[RuHCl(CO)(PPh_3)_3]$ with different yield and coordination behavior. NS coordination of the ligand with the formation of an unusual four-membered ring (VIII) was found in complex **1**, and ONS coordination (VI) with five- and six-membered-ring formation was found in complex **2**. According to the report of Bhattacharya et al., if the intramolecular hydrogen bonding and the bulkiness were the only responsible factors, we could have obtained only a product of type VIII.[50,53] However, we obtained a complex of type VI in higher yield as compared with type VIII. From this, it is concluded that the aforementioned factors are not the only responsible factors in determining the coordination behavior of thiosemicarbazones and there may be some other factors and/or their collective influence in directing them.

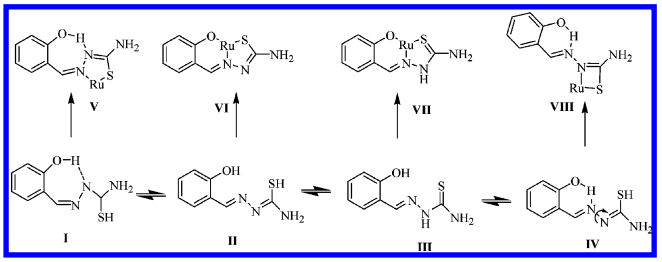

Electrochemistry. The complexes **1** and **2** were electroactive in the sweep range ±2.00 V. The cyclic voltammogram of **1** showed a reversible one-electron-oxidation response $E_{1/2}$(oxi) at 0.725 V with a peak to peak separation of 50 mV and quasi-reversible reduction at −0.480 V with a peak to peak separation of 200 mV (Table S2, Supporting Information). These quasi-reversible reduction peaks can be assigned to a Ru(II)/Ru(I) process. In addition, complex **1** showed both quasi-reversible ligand oxidation and reduction with $E_{1/2}$ at 1.125 and −1.385 V and peak to peak separations of 250 and 130 mV, respectively (Figures S3 and S4, Supporting Information). Complex **2** exhibited quasi-reversible oxidation at 0.549 V with a peak to peak separation of 332 mV and reversible reduction corresponding to Ru(II)/Ru(I) at −0.460 V with a peak to peak separation of 80 mV. The reason for the quasi-reversible electron transfer process may be due to slow electron transfer or the adsorption of the complex onto the electrode surface.[55]

dx.doi.org/10.1021/om300914n | *Organometallics* 2012, 31, 8323−8332

From current electrochemical investigations, it is concluded that the ligand [H_2-(Sal-tsc)] can stabilize the lower and higher oxidation states of the metal.

DNA Binding Studies. UV absorption titration experiments were carried out to study the DNA binding properties of the new Ru(II) complexes **1** and **2**. The absorption spectra of the new complexes at constant concentration (10 μM) in the presence of different concentrations of CT-DNA (0.05−0.50 μM) are given in Figure 5. The absorption spectra of complex **1** at 404 nm showed hypochromism (A = 0.0501−0.0426) without a wavelength shift in the absorption maxima. As shown in Figure 5, the addition of CT-DNA to complex **2** also led to isosbestic spectral changes with an isosbestic point at 304 nm. The observed hyperchromic effect with blue shift in the intraligand band suggested that the new ruthenium(II) complexes bind to CT-DNA by external contact, possibly due to electrostatic binding.[56]

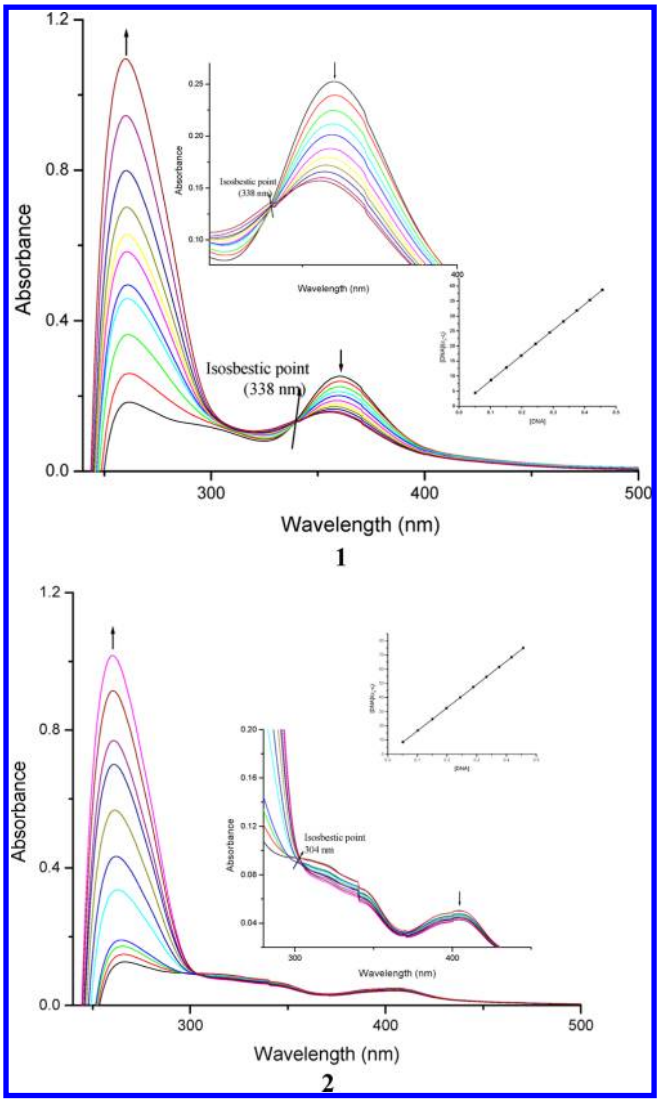

Figure 5. Absorption titration spectra of **1** and **2** with increasing concentrations (0.05−0.5 μM) of CT-DNA (phosphate buffer, pH 7). The inset shows binding isotherms with CT-DNA.

mainly consist of two resolved bands (intraligand (IL) and CT transitions) centered at 262 nm (IL) and 360 nm (CT). As the DNA concentration is increased, a hyperchromism (A = 0.2598−1.0963) with a blue shift of 2 nm was observed in the intraligand band. The CT band at 360 nm showed hypochromism (A = 0.2525−0.1571) with a 5 nm blue shift in the absorption maxima. In addition, the binding of complex **1** to CT DNA led to isosbestic spectral changes with an isosbestic point at 338 nm. For complex **2**, upon addition of DNA, the intraligand band at 267 nm exhibited hyperchromism (A = 0.1264−1.0167) with a blue shift of 7 nm. The CT band

The intrinsic binding constant K_b is a useful tool to determine the magnitude of the binding strength of compounds with CT-DNA. It can be determined by monitoring the changes in the absorbance in the IL band at the corresponding λ_{max} value with increasing concentration of DNA and is given by the ratio of slope to the y intercept in plots of [DNA]/($\varepsilon_a - \varepsilon_f$) versus [DNA] (insets in Figure 5). From the binding constant values (Table 2), it is inferred that both the complexes bind with CT-DNA more efficiently.

Table 2. Binding Constant for Interaction of Complexes with CT-DNA

system	K_b (10^5 M^{-1})
CT-DNA + **1**	5.5977
CT-DNA + **2**	5.5815

Emission spectral studies were carried out to know more on the binding nature of metal complexes to DNA. Complex **1** had a fluorescence emission at 412 nm (Figure 6), while addition of CT DNA to the complex solution resulted in hyperchromism with an increase in intensity (I = 45.21−79.38) without any shift in the absorption maxima. However, in complex **2**, hypochromism was observed with a decrease in intensity at 469 nm (41.73−33.73). The enhanced fluorescence intensity observed for complex **1** symbolizes electrostatic binding of DNA. However, the marked decrease in the fluorescence intensity of complex **2** indicates the intercalative binding mode of DNA.

The results obtained from the above experiments suggested that both the compounds can bind with CT-DNA. However, the exact mode of binding cannot be proposed by these studies. Hence, ethidium bromide displacement studies were carried out. Ethidium bromide competitive binding experiments using new ruthenium(II) complexes **1** and **2** as quenchers may give further information about the binding of these complexes to DNA. EB emits intense fluorescence light in the presence of DNA, due to its strong intercalation between adjacent DNA base pairs. The quenching extent of fluorescence of EB bound to DNA is used to determine the extent of binding of metal complexes to DNA. When complexes **1** and **2** were added to DNA pretreated with EB, the DNA induced emission intensity at 602 nm was decreased (Figure 7). This indicated that the complexes could replace EB from the DNA-EB system. The Stern−Volmer quenching constants K_{sv}, obtained as a slope from the plot of I_0/I vs [Q] (Figure 7, inset), were found to be 1.65×10^3 and 8.72×10^3 M^{-1}, respectively, for complexes **1** and **2**. The results obtained suggested that the complex **2** has relatively high magnitude of binding than complex **1**.

Further, the apparent DNA binding constants (K_{app}) were calculated using eq 3, where [complex] is the value at 50%

$$K_{EB}[EB] = K_{app}[complex] \quad (3)$$

dx.doi.org/10.1021/om300914n | Organometallics 2012, 31, 8323−8332

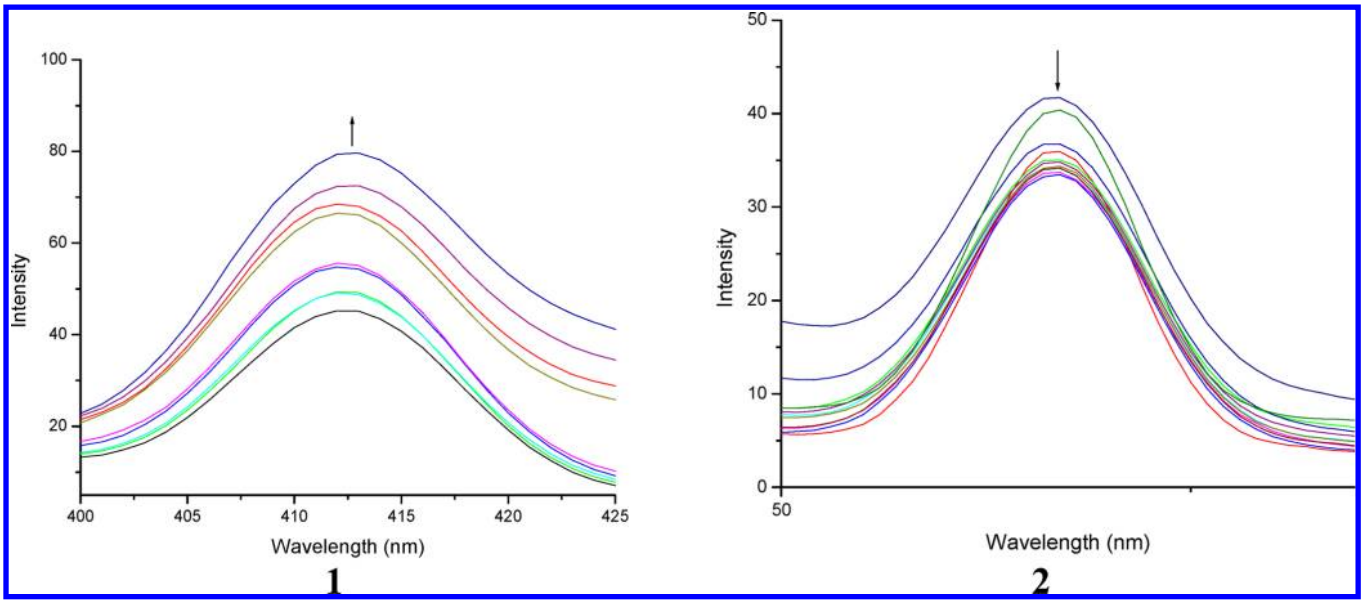

Figure 6. Changes in the emission spectra of **1** and **2** with increasing concentrations (0.05−0.5 μM) of CT-DNA (phosphate buffer, pH 7).

reduction in the fluorescence intensity of EB, K_{EB} (1.0×10^7 M^{-1}) is the DNA binding constant of EB, and [EB] is the concentration of EB (12 μM). K_{app} values were 1.98×10^5 and 10.46×10^5 M^{-1} for complexes **1** and **2**, respectively. From these experimental data, it is seen that the ruthenium(II) complex **2** replaces EB more effectively than **1**, which is in agreement with the results observed from the electronic absorption spectra. Since these changes indicate only one kind of quenching process, it may be concluded that both complexes can bind to DNA via the intercalation mode. Furthermore, the observed quenching constants and binding constants of the new complexes **1** and **2** suggest that the interaction of both complexes with DNA should be intercalative.[57]

MTT (3-(4,5-Dimethylthiazol-2-yl)-2,5-diphenyltetrazolium Bromide) Assay. The cytotoxic effect of the new ruthenium(II) complexes **1** and **2** and the ligand on the proliferation of human lung cancer and liver cancer cell lines A549 and HepG2 were assayed by MTT (3-(4,5-dimethylthiazol-2-yl)-2,5-diphenyltetrazolium bromide assay). From the results, it is found that complex **2** exhibited higher antiproliferative activity than **1** (Figure S5, Supporting Information). The IC_{50} values were found to be 26 ± 1.03 and 23 ± 0.99 for A549 and 23 ± 1.01 and 20 ± 1.21 for HepG2 cells, respectively, for complexes **1** and **2**. In comparison with the conventional standard cisplatin, complex **2** was found to have a lower IC_{50} value for the A549 cell line. However, for HepG2, both complexes have IC_{50} values higher than that for cisplatin. In order to assess whether the complexes exhibited their cytotoxic activity through the induction of oxidative stress, we analyzed the cell viability in the presence of an antioxidant, glutathione (Figure 8). The results of the present study indicated that the cell viability was significantly increased in the presence of glutathione in the cells treated with the complexes. This in turn supports the notion that the newly synthesized complexes exhibited their cytotoxic activities through ROS generation and thereby oxidative stress.

Lactate Dehydrogenase Release. When cancer cell lines A549 and HepG2 were treated with the new ruthenium(II) complexes treated for a period of 48 h, a significant increase of LDH release in the culture medium was observed (Figure 9). This indicates the efficiency of new complexes in inducing cell death by collapsing the membrane integrity. LDH is a stable cytoplasmic enzyme that is released into the culture medium following loss of membrane integrity and serves as a general means to assess cytotoxicity resulting from chemical compounds or environmental toxic factors. The significant increase of LDH level in the culture supernatant confirmed the cytotoxic effect of the newly synthesized complexes on lung and liver cancer cell lines. This study has highlighted how the complexes enhance cell death via a mechanism which is dependent on the induction of oxidative stress. Oxidative stress damages the membrane lipids, thereby leading to the destruction of membrane integrity. This in turn may lead to the LDH release from the cells treated with the complexes. The induction of LDH release was found to be higher for complex **2** than for **1**. These results are comparable with our earlier reports and those of Alia et al., concerning the significant release of LDH leakage into the culture medium, which confirms the cytotoxic effect induced by the complexes.[48,58−60]

Nitric Oxide Assay. The nitric oxide (NO) assay is also an important measure of cytotoxicity, as NO has been shown to directly inhibit methionine adenosyl transferase, leading to glutathione depletion, and its reaction with superoxide generates the strong oxidant peroxynitrite, which can initiate lipid peroxidation or cause a direct inhibition of the mitochondrial respiratory chain.[61] In the present study NO release by the new ruthenium(II) complexes was evaluated using A549 and HepG2 cells. The quantification of the nitrite produced in the cell media by the Griess assay is an indirect but cost-effective measurement of the amount of NO produced by the cells. It is interesting to note that both complexes were found to release more NO than the control, and **2** was found to be the more effective complex (Figure 10). The results of the nitric oxide assay support the concept that the complex-induced cell death is mediated by reactive oxygen species generation.

Cellular Uptake Study. The intracellular uptake of a specific drug plays a vital role in ameliorating several diseases. Since the IC_{50} values are critical when comparing normal cells in the human body, the present study was focused on the

dx.doi.org/10.1021/om300914n | *Organometallics* 2012, 31, 8323−8332

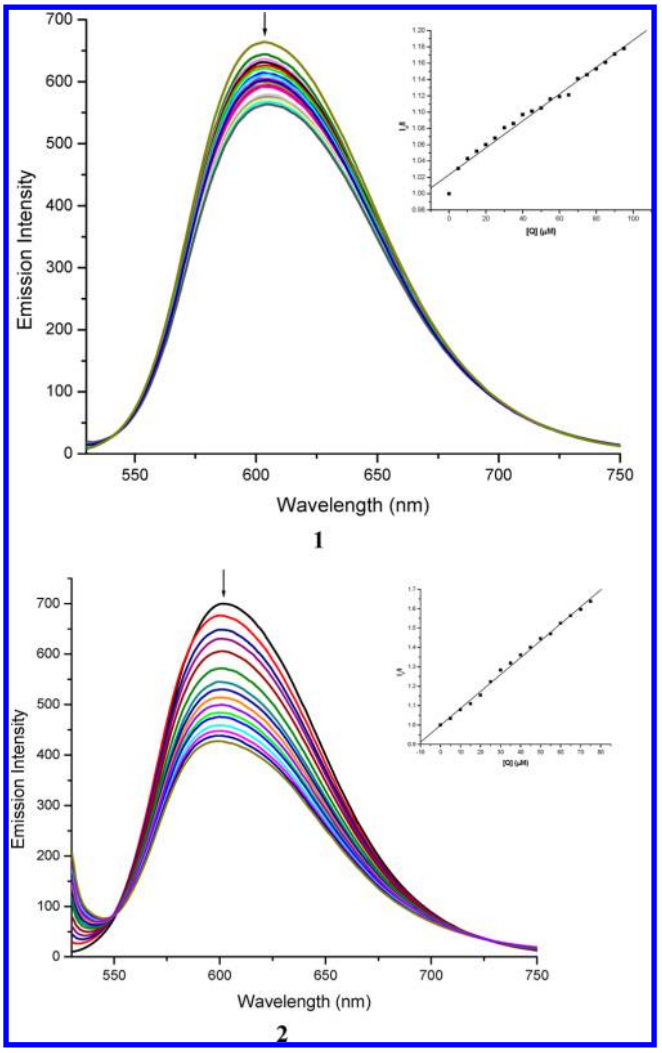

Figure 7. Emission spectra of EB bound to DNA in the presence of complexes **1** and **2** in Tris-HCl buffer (pH 7). Arrows indicate the intensity changes upon increasing concentration of the complexes. Inset: fluorescence quenching curve of DNA-bound EB with the complexes.

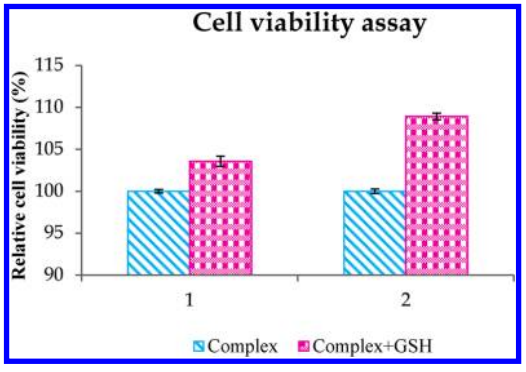

Figure 8. Cell viability assay of the complexes in presence of glutathione.

concentrations which showed 50% inhibition for A549 and HepG2 cell lines. The intracellular concentrations of complexes **1** and **2** were determined as described in the Experimental Section. The intracellular concentrations of complexes **1**, **2** and ligand after an incubation period of 4 h were found to be 61.53 and 69.56%, 54.34 and 62.5% and 27.35 and 31.25%,

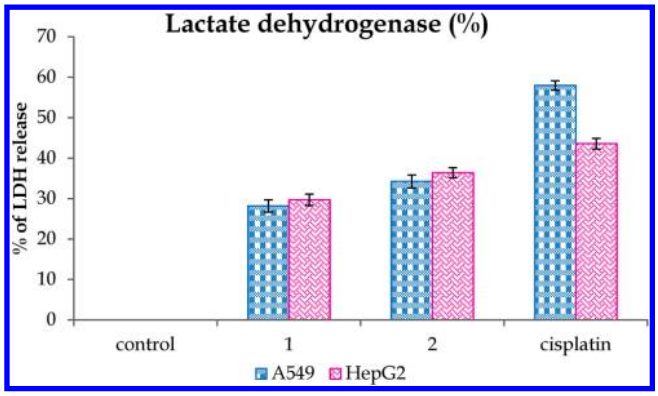

Figure 9. Percentage of lactate dehydrogenase released by the human cancer cell lines A549 and HepG2 after an incubation period of 48 h with complexes **1** and **2**. Error bars represent the standard mean error (n = 6).

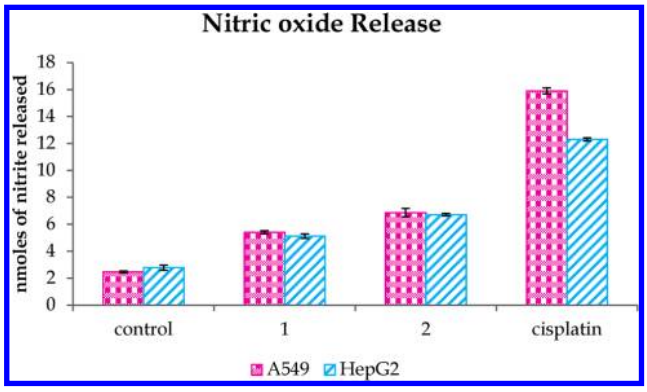

Figure 10. Nitrite released (in nmol) by the human cancer cell lines A549 and HepG2 after an incubation period of 48 h with complexes **1** and **2**. Error bars represent the standard mean error (n = 6).

respectively, for A549 and HepG2 cell lines (Figure 11). It is obvious from the results that, even at low concentrations of the

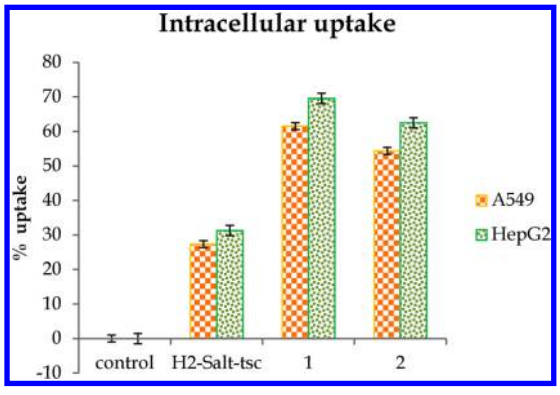

Figure 11. Percentage of intracellular uptake of complexes **1** and **2** by human cancer cell lines A549 and HepG2 after an incubation period of 2 h. Error bars represent the standard mean error (n = 6).

complexes, they are cytotoxic to the lung and liver cancer cells when they are completely absorbed by the cell; in particular, the uptake level of complex **1** by both cell lines is higher than that of **2**. The uptake levels were dependent on the dose of each complex used. This also indicates that their cytotoxicities as determined by the MTT assay were not disproportionately influenced by the complexes having different cellular uptake

dx.doi.org/10.1021/om300914n | *Organometallics* 2012, 31, 8323−8332

levels. Results in their percentage uptake are shown as mean ± SD (n = 9), in three separate experiments performed in triplicate.

CONCLUSIONS

In an effort to determine the coordination behavior of thiosemicarbazones, the reaction of salicylaldehydethiosemicarbazone [H_2-(Sal-tsc)] with [$RuHCl(CO)(PPh_3)_3$] has been carried out and discussed in this article. The stoichiometric reaction afforded two different complexes having different structural features, and they were characterized by various spectral, analytical, X-ray crystallographic, and cyclic voltammetric methods. It is interesting to note that one of the complexes obtained (**1**) has thiosemicarbazone coordinated as NS through the N(2) nitrogen and thiolate sulfur by forming an unusual four-membered ring, whereas in complex **2**, the same ligand coordinated as an ONS dibasic tridentate donor. Since these two new ruthenium complexes containing a biologically active thiosemicarbazone moiety have different coordination modes, an attempt was made to compare their modes of chelation with their potential biological activities. For that purpose, they were subjected to CT-DNA binding, cytotoxicity (MTT, lactate dehydrogenase (LDH), and NO release in human carcinoma cell lines A549 and HepG2), and cellular uptake studies. The results showed that complex **2** has an activity higher than that of **1**, and this may be due to the strong chelation and increased electron delocalization in **2** increasing the lipophilic character of the metal ion into the cells in comparison to **1**. Further studies remain to determine the coordination behavior of thiosemicarbazones and exact molecular mechanism of cytotoxicity.

ASSOCIATED CONTENT

Supporting Information

CIF files, tables, and figures giving crystallographic data for [$Ru(H\text{-}Sal\text{-}tsc)(CO)Cl(PPh_3)_2$] (**1**) and [$Ru(Sal\text{-}tsc)(CO)(PPh_3)_2$] (**2**), ^{31}P NMR spectra and cyclic voltammograms of **1** and **2**, and results of a cell proliferation (MTT) assay. This material is available free of charge via the Internet at http://pubs.acs.org. Crystallographic data for **1** and **2** have also been deposited at the Cambridge Crystallographic Data Centre as supplementary publications (CCDC Nos. 857206 and 857205). The data can be obtained free of charge at www.ccdc.cam.ac.uk/conts/retrieving.html or from the Cambridge Crystallographic Data Centre, 12 Union Road, Cambridge CB2 1EZ, U.K. (fax, +44-1223/336-033; e-mail, deposit@ccdc.cam.ac.uk).

AUTHOR INFORMATION

Corresponding Author

*Tel: +91-422-2428319. Fax: +91-422-2422387. E-mail: rpnchemist@gmail.com (R.P.); k_natraj6@yahoo.com (K.N.).

Notes

The authors declare no competing financial interest.

ACKNOWLEDGMENTS

We gratefully acknowledge the Council of Science and Industrial Research, New Delhi, India, and Department of Science and Technology, New Delhi, India, for financial assistance.

REFERENCES

(1) (a) Campbell, M. J. M. *Coord. Chem. Rev.* **1975**, *15*, 297. (b) Casas, J. S.; Garcia-Tasende, M. S.; Sordo, J. *Coord. Chem. Rev.* **2000**, *209*, 197.
(2) (a) Basuli, F.; Peng, S. M.; Bhattacharya, S. *Inorg. Chem.* **1997**, *36*, 5645. (b) Basuli, F.; Ruf, M.; Pierpont, C. G.; Bhattacharya, S. *Inorg. Chem.* **1998**, *37*, 6113. (c) Basuli, F.; Ruf, M.; Pierpont, C. G.; Bhattacharya, S. *Inorg. Chem.* **2000**, *39*, 1120. (d) Pal, I.; Basuli, F.; Mak, T. C. W.; Bhattacharya, S. *Angew. Chem., Int. Ed. Engl.* **2001**, *113*, 3007. (e) Archaryya, R.; Basuli, F.; Peng, S. M.; Lee, G. H.; Falvello, L. R.; Bhattacharya, S. *Inorg. Chem.* **2006**, *45*, 1252. (f) Ze-hua, L.; Chung-Ying, D.; Ji-hui, L.; Young-jiang, L.; Yu-hua, M.; X-Zeng, Y. *New J. Chem.* **2000**, *24*, 1057. (g) Prabhakaran, R.; Kalaivani, P.; Renukadevi, S. V.; Huang, R.; Senthilkumar, K.; Karvembu, R.; Natarajan, K. *Inorg. Chem.* **2012**, *51*, 3525.
(3) West, D. X.; Swearingen, J. K.; Valdes-Martinez, J.; Hernandez-Ortega, S.; El-Sawaf, A. K.; van Meurs, F.; Castineiras, A.; Garcia, I.; Bermejo, E. *Polyhedron* **1999**, *18*, 2919.
(4) Tarasconi, P.; Capacchi, S.; Pelosi, G.; Cornia, M.; Albertini, R.; Bonati, A.; Dall'Aglio, P.; Lunghi, P.; Pinelli, S. *Bioorg. Med. Chem.* **2000**, *8*, 157.
(5) Ghazy, S. E.; Kabil, M. A.; El-Asmy, A. A.; Sherief, Y. A. *Anal. Lett.* **1996**, *29*, 1215.
(6) Dilworth, J. R.; Cowley, A. H.; Donnelly, P. S.; Gee, A. D.; Heslop, J. M. *Dalton Trans.* **2004**, 2404.
(7) Bruijnincx, P. C. A.; Sadler, P. J. *Adv. Inorg. Chem.* **2009**, *61*, 1.
(8) Dyson, P. J.; Sava, G. *Dalton Trans.* **2006**, 1929.
(9) Allardyce, C. S.; Dorcier, A.; Scolaro, C.; Dyson, P. J. *Appl. Organomet. Chem.* **2005**, *19*, 1.
(10) Bratsos, I.; Jedner, S.; Gianferrara, T.; Alessio, E. *Chimia* **2007**, *61*, 692.
(11) Rosenberg, B.; Vancamp, L.; Trosko, J. E.; Mansour, V. H. *Nature* **1969**, *222*, 385.
(12) Brown, S. J.; Chow, C. S.; Lippard, S. J. In *Encyclopedia of Inorganic Chemistry*; King, R. B., Ed.; Wiley: West Sussex, England, 1994; p 3305.
(13) Durig, J. R.; Danneman, J.; Behnke, W. D.; Mercer, E. E. *Chem.-Biol. Interact.* **1976**, *13*, 287.
(14) Clarke, M. J. *Met. Ions Biol. Syst.* **1980**, *11*, 231.
(15) Clarke, M. J.; Zhu, F.; Frasca, D. R. *Chem. Rev.* **1999**, *99*, 2511.
(16) Novakova, O.; Kasparkova, J.; Vrana, O.; Vanvliet, P. M.; Reedijk, J.; Brabec, V. *Biochemistry* **1995**, *34*, 12369.
(17) Vanvliet, P. M.; Toekimin, S. M. S.; Haasnoot, J. G.; Reedijk, J.; Novakova, O.; Vrana, O.; Brabec, V. *Inorg. Chim. Acta* **1995**, *231*, 57.
(18) Vilaplana, R.; Romero, M.; Quiros, M.; Salas, J.; Gonzalez-Vilches, F. *Met.-Based Drugs* **1995**, *2*, 211.
(19) Chatterjee, D.; Mitra, A.; De, G. S. *Platinum Met. Rev.* **2006**, *50*, 2.
(20) Alessio, E.; Mestroni, G.; Nardin, G.; Attia, W. M.; Calligaris, M.; Sava, G.; G. Zorzet, G. *Inorg. Chem.* **1988**, *27*, 4099.
(21) Sava, G.; Pacor, S.; Zorzet, S.; Alessio, E.; Mestroni, G. *Pharmacol. Res.* **1989**, *21*, 617.
(22) Coluccia, M.; Sava, G.; Loseto, F.; Nassi, A.; Bocarelli, A.; Giordano, D.; Alessio, E.; Mestroni, G. *Eur. J. Cancer* **1993**, *29*, 1873.
(23) Velders, A. H.; Kooijman, H.; Spek, A. L.; Haasnoot, J. G.; de Vos, D.; Reedijk, J. *Inorg. Chem.* **2000**, *39*, 2966.
(24) Hotze, A. C. G.; Caspers, S. E.; de Vos, D.; Kooijman, H.; Spek, A. L.; Flamigni, A.; Bacac, M.; Sava, G.; Haasnoot, J. G.; Reedijk, J. *J. Biol. Inorg. Chem.* **2004**, *9*, 354.
(25) Kelman, A. D.; Clarke, M. J.; Edmonds, S. D.; Peresie, H. J. *J. Clin. Hematol. Oncol.* **1977**, *7*, 274.
(26) Allardayce, C. S.; Dyson, P. J. *Platinum Met. Rev.* **2001**, *45*, 62.
(27) Kostova, J. *Curr. Med. Chem.* **2006**, *13*, 1085.
(28) Purohit, S.; Kolay, A. P.; Prasad, L. S.; Manoharan, P. T.; Ghosh, S. *Inorg. Chem.* **1989**, *28*, 3735.
(29) Klayman, D. L.; Brtosevich, J. F.; Griffin, T. S.; Mason, C. J.; Scovill, J. P. *J. Med. Chem.* **1997**, *22*, 855.
(30) Ahmed, N.; Levision, J. J.; Robinson, S. D.; Uttley, M. F. *Inorg. Synth.* **1974**, *15*, 48.

(31) Vogel, A. I. *Textbook of Practical Organic Chemistry*, 5th ed.; Longman: London, 1989; p 268.
(32) (a) Blessing, R. H. *Acta Crystallogr.* **1995**, *A51*, 33. (b) Blessing, R. H. *Cryst. Rev.* **1987**, *1*, 3. (c) Blessing, R. H. *J. Appl. Crystallogr.* **1989**, *22*, 396.
(33) Sheldrick, G. M. *SHELXTL Version 5.1, An Integrated System for Solving, Refining and Displaying Crystal Structures from Diffraction Data*; Siemens Analytical X-ray Instruments, Madison, WI, 1990.
(34) Sheldrick, G. M. *SHELXL-97, A Program for Crystal Structure Refinement, Release 97-2*; Institut fur Anorganische Chemie der Universitat Gottingen, Tammanstrasse 4, D-3400 Gottingen, Germany, 1998.
(35) Wolfe, A.; Shimer, G. H.; Meehan, T. *Biochemistry* **1987**, *26*, 6392.
(36) Cohen, G.; Eisenberg, H. *Biopolymers* **1969**, *8*, 45.
(37) Mossman, T. *J. Immunol. Methods* **1983**, *65*, 55.
(38) Wacker, W. E. C.; Ulmer, D. D.; Valee, B. L. *J. Med.* **1956**, *255*, 449.
(39) Stueher, D. J.; Marletta, M. A. *J. Immunol.* **1987**, *139*, 518.
(40) Xiong, X. B.; Ma, Z.; Lai, R.; Lavasanifar, A. *Biomaterials* **2010**, *31*, 757.
(41) Prabhakaran, R.; Jayabalakrishnan, C.; Krishnan, V.; Pasumpon, K.; Sukanya, D.; Bertagnolli, H.; Natarajan, K. *Appl. Organomet. Chem.* **2006**, *20*, 203.
(42) Prabhakaran, R.; Karvembu, R.; Hashimoto, T.; Shimizu, K.; Natarajan, K. *Inorg. Chim. Acta* **2005**, *358*, 2093.
(43) Prabhakaran, R.; Renukadevi, S. V.; Karvembu, R.; Huang, R.; Mautz, J.; Huttner, G.; Subhaskumar, R.; Natarajan, K. *Eur. J. Med. Chem.* **2008**, *43*, 268.
(44) Prabhakaran, R.; Renukadevi, S. V.; Karvembu, R.; Huang, R.; Zeller, M.; Natarajan, K. *Inorg. Chim. Acta* **2008**, *361*, 2547.
(45) Prabhakaran, R.; Kalaivani, P.; Jayakumar, R.; Zeller, M.; Hunter, A. D.; Renukadevi, S. V.; Ramachandran, E.; Natarajan, K. *Metallomics* **2011**, *3*, 42.
(46) Karvembu, R.; Hemalatha, S.; Prabhakaran, R.; Natarajan, K. *Inorg. Chem. Commun.* **2003**, *6*, 486.
(47) Tojal, J. G.; Dizarro, J. L.; Orad, A. G.; Sanz, A. R. P.; Ugalda, M.; Diaz, A. A.; Serra, J. L.; Arriortua, M. I.; Rojo, T. *J. Inorg. Biochem.* **2001**, *86*, 627.
(48) Kalaivani, P.; Prabhakaran, R.; Dallemer, F.; Poornima, P.; Vaishnavi, E.; Ramachandran, E.; Vijaya Padma, V.; Renganathan, R.; Natarajan, K. *Metallomics* **2012**, *4*, 101.
(49) Rodrigues, C.; Batista, A. A.; Aucélio, R. Q.; Teixeira, L. R.; Visentin, L. C.; Beraldo, H. *Polyhedron* **2008**, *27*, 3061.
(50) Basuli, F.; Ruf, M.; Pierpont, C. G.; Bhattacharya, S. *Inorg. Chem.* **1998**, *37*, 6113.
(51) (a) Chellan, P.; Land, K. M.; Shokar, A.; Au, A.; Clavel, C. M.; Dyson, P.; Kock, C.; Smith, P. J.; Chibale, K.; Smith, G. S. *Organometallics* **2012**, *31*, 5791. (b) Ali, A. A.; Nimir, H.; Aktas, C.; Huch, V.; Rauch, U.; Schafer, K. H.; Veith, M. *Organometallics* **2012**, *31*, 2256. (c) Carreira, M.; Sanjuan, R. C.; Sanau, M.; Marzo, I.; Cont, M. *Organometallics* **2012**, *31*, 5772.
(52) Prabhakaran, R.; Anantharaman, S.; Thilagavathi, M.; Kaveri, M. V.; Kalaivani, P.; Karvembu, R.; Dharmaraj, N.; Bertagnolli, H.; Dallemer, F.; Natarajan, K. *Spectrochim. Acta, Part A* **2011**, *78*, 844–853.
(53) (a) Basuli, F.; Peng, S. M.; Bhattacharya, S. *Inorg. Chem.* **1997**, *36*, 5645. (b) Basuli, F.; Peng, S. M.; Bhattacharya, S. *Inorg. Chem.* **2000**, *39*, 1120. (c) Basuli, F.; Peng, S. M.; Bhattacharya, S. *Inorg. Chem.* **2001**, *40*, 1126.
(54) Prabhakaran, R.; Huang, R.; Karvembu, R.; Jayabalakrishnan, C.; Natarajan, K. *Inorg. Chim. Acta* **2007**, *360*, 691.
(55) Wallace, A. W.; Murphy, W. R.; Peterson, J. D. *Inorg. Chim. Acta* **1989**, *166*, 47.
(56) (a) Long, E. C.; Barton, J. K. *Acc. Chem. Res.* **1990**, *23*, 271. (b) Pasternack, R. F.; Gibbs, E. J.; Villafranca, J. J. *Biochemistry* **1983**, *22*, 251.
(57) Kalaivani, P.; Prabhakaran, R.; Ramachandran, E.; Dallemer, F.; Paramaguru, G.; Renganathan, R.; Poornima, P.; Vijaya Padma, V.; Natarajan, K. *Dalton Trans.* **2012**, *41*, 2486.
(58) Li, Y.; Yang, Z. Y.; Wu, J. C. *Eur. J. Med. Chem.* **2010**, *45*, 5692.
(59) Prabhakaran, R.; Kalaivani, P.; Poornima, P.; Dallemer, F.; Paramaguru, G.; Vijaya Padma, V.; Renganathan, R.; Huang, R.; Natarajan, K. *Dalton Trans.* **2012**, *41*, 9323.
(60) Alia, M.; Ramos, S.; Mateos, R.; Serrano, A. B. G.; Bravo, L.; Goya, L. *Toxicol. Appl. Pharmacol.* **2006**, *212*, 110.
(61) Yu, L.; Gengaro, P. E.; Niederberger, M.; Burke, T. J.; Schriert, R. W. *Proc. Natl. Acad. Sci. U.S.A.* **1994**, *91*, 1691.

NOTE ADDED AFTER ASAP PUBLICATION

In the version of this paper published on Nov 28, 2012, ref 44 had the wrong volume and page information. In addition, ref 58 was a duplicate of ref 48. In the version published on Dec 10, 2012, ref 44 is correct and ref 58 has been deleted; the references following the original ref 58 have been renumbered and their citations in the text updated.